European Journal of Inorganic Chemistry

EurJIC
European Journal of Inorganic Chemistry

Chemistry Europe
European Chemical Societies Publishing

RESEARCH ARTICLE OPEN ACCESS

Dinuclear Rhodium(I)–*N*-Heterocyclic Carbene Complexes as Alkyne Hydropyridonation Catalysts

Belinda Español-Sánchez[1] | Mert Olgun Karataş[1,2] | Andrea Di Giuseppe[3] | Ulugbek Togaev[1,4] | Vincenzo Passarelli[1] | Luis A. Oro[1] | Jesús J. Pérez-Torrente[1] | Ricardo Castarlenas[1]

[1]Instituto de Síntesis Química y Catálisis Homogénea (ISQCH), Departamento de Química Inorgánica, CSIC-Universidad de Zaragoza, Zaragoza, Spain | [2]Department of Chemistry, İnönü University, Malatya, Türkiye | [3]Dipartimento di Scienze Fisiche e Chimiche, Università dell'Aquila, L'Aquila, Italy | [4]The Engineering School, Central Asian University, Tashkent, Uzbekistan

Correspondence: Ricardo Castarlenas (rcastar@unizar.es)

Received: 13 November 2025 | **Revised:** 10 December 2025 | **Accepted:** 11 December 2025

Keywords: halogen bond | hydroamidation | hydropyridonation | N-heterocyclic carbene | shim chemistry

ABSTRACT

A series of new Rh^{I}–*N*-Heterocyclic carbene dinuclear complexes of type $[Rh(\mu\text{-Cl})(\eta^2\text{-coe})(NHC)]_2$, containing IPr^{BIAN}, IPr^{Cl}, and IPr* ligands, has been prepared. The crystal structure of the IPr^{Cl} functionalized rhodium–dinuclear complex reveals an intermolecular Cl···Cl halogen bond. The chlorido-bridges can be cleaved by pyridine to afford the corresponding mononuclear derivatives $RhCl(\eta^2\text{-coe})(NHC)(py)$. These complexes are efficient alkyne hydropyridonation catalysts, with the IMes complex exhibiting the highest reactivity within the series.

1 | Introduction

The remarkable success of organometallic catalysis in modern synthetic chemistry undeniably stems from the rational design of catalyst architectures guided by mechanistic insight and structure–activity relationships [1–4]. Among the diverse classes of ligands investigated, *N*-heterocyclic carbenes (NHCs) have emerged as particularly significant because of their unique stereoelectronic properties, which can be readily tailored through structural modification [5–11]. Notably, the incorporation of NHCs into rhodium-based complexes has enabled the development of a wide array of catalytic systems with broad applicability [12–17]. Typically, the RhX(NHC)(cod) (cod = cyclooctadiene) platform has been the most successful entry for incorporating newly designed NHC architectures into the metal coordination sphere, owing to the synthetic accessibility and robustness of the resulting complexes [18–23]. However, the strong coordination of the diene ligand may hinder catalytic activity in transformations that require the rapid generation of vacant coordination sites. As an alternative, dinuclear complexes of the type $[Rh(\mu\text{-X})(\eta^2\text{-olefin})(NHC)]_2$ provide more active precursors, as they undergo faster initiation through bridge cleavage and mono-olefin decoordination, albeit at the expense of catalyst stability [24–37]. Following the seminal synthetic studies by the groups of Nolan [24, 25], James [26, 27], and Crudden [28–30], further efforts have been devoted to the preparation of this type of well-defined complexes, incorporating structural modifications at either the NHC or the olefin ligands (Chart 1) [31–37]. Notably, the advantages associated with dinuclear architectures have also been demonstrated in related M-NHC chlorido-bridged systems of other transition metals, such as $[Pd(\mu\text{-Cl})Cl(NHC)]_2$ [38], $[Ni(\mu\text{-Cl})(NHC)]_2$ [39], $[FeCl(\mu\text{-Cl})(NHC)]_2$ [40], $[Ru(\mu\text{-Cl})_3(NHC)_2]_2^+$ [41], $[CoCl(\mu\text{-Cl})(NHC)]_2$ [42], or $[MnCl(\mu\text{-Cl})(NHC)]_2$ [43].

Alkyne functionalization holds a pivotal role in carbon–heteroatom coupling reactions [44–46]. In particular, metal-catalyzed alkyne hydroamidation provides a straightforward approach to elaborated organic scaffolds [47]. Unlike other X-H addition substrates, amides display versatile reactivity, enabling the formation of either carbon–nitrogen or carbon–oxygen bonds. However, the chemoselectivity is largely driven by nitrogen nucleophilic attack on the triple bond, typically proceeding via an anti-Markovnikov pathway to

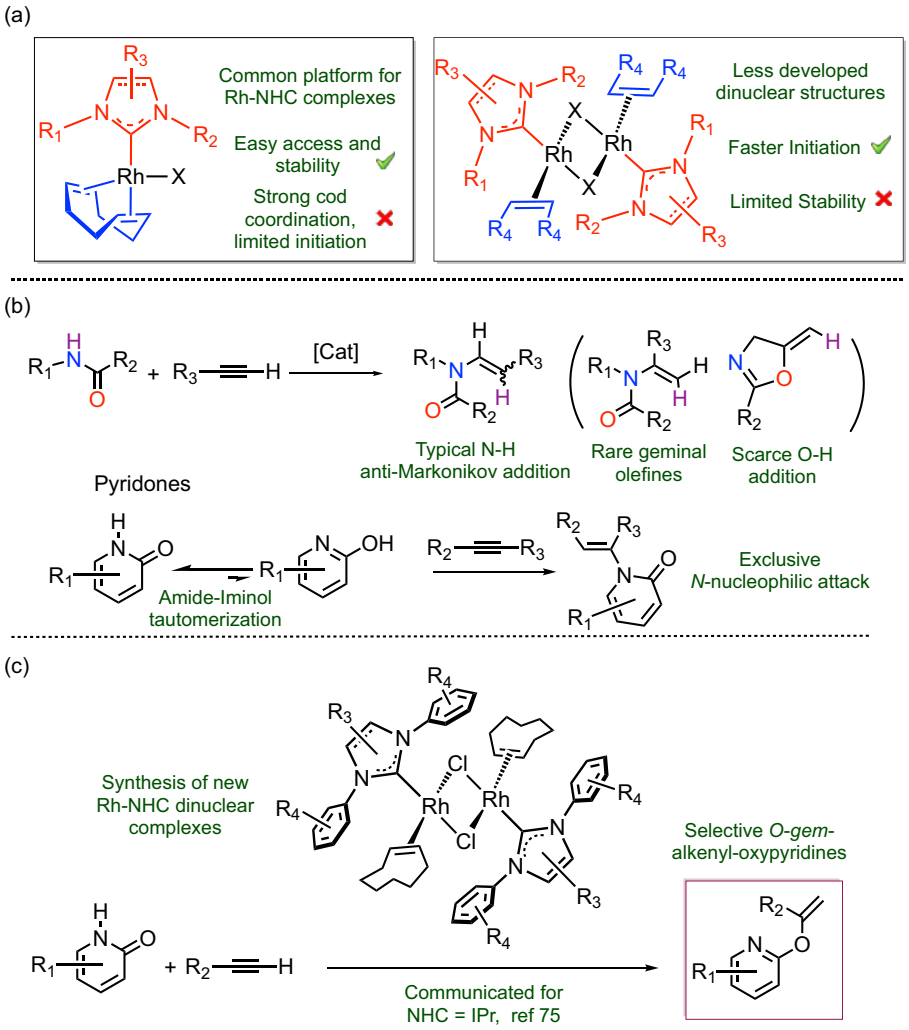

CHART 1 | (a) Comparison of Rh^{I}–NHC platforms. (b) Selectivity in alkyne hydroamidation and hydropyridonation. (c) Our approach: Synthesis of new dinuclear Rh–NHC complexes as catalysts for selective formation of *O-gem*-alkenyloxypyridines.

afford *E*/*Z*-enamides [48–51]. In contrast, the formation of geminal counterparts has only recently been achieved through the use of dioxazolones as amide surrogates [52]. Moreover, *O*-nucleophilic attack is considerably less common and has been reported exclusively in the intramolecular cyclization of propargylamides [53, 54].

Pyridones constitute a unique class of amides. A defining feature of these molecules is the amide–iminol tautomerization equilibrium [55], which confers distinctive reactivity [56–59] and opens new avenues for chemoselective transformations [60]. The addition of pyridones to alkynes has been demonstrated with substrates bearing strong electron-withdrawing [61–63] or electron-donating [64] groups, as well as internal alkynes [65–71], affording *E*- [62], *Z*- [63], or *gem*-alkenyl [61, 64] pyridone derivatives. However, all reported alkyne hydropyridonations proceed exclusively via *N*-nucleophilic attack. As far as we are aware, only three examples of O–H addition of pyridones to carbon–carbon multiple bonds have been reported [72–74], involving either allenes [72, 73] or a styrene coupling partner [74]. Actually, in the latter two cases, some uncertainty remains regarding the possible formation of the *N*-alkylated derivative. In this context, we have recently reported a dinuclear Rh–NHC catalyst $[Rh(\mu\text{-}Cl)(\eta^2\text{-coe})(IPr)]_2$ (**1**) {coe = cyclooctene, IPr = 1,3-bis (2,6-diisopropylphenyl)imidazolin-2-carbene} capable of overturning the inherent *N*-selectivity of pyridones in alkyne hydropyridonation, thereby enabling chemoselective *O*-alkenylation [75]. Notably, this catalytic system also exhibits specific Markovnikov-regioselectivity, furnishing geminal alkenylated products exclusively.

Building on the principle of rational catalyst design driven by mechanistic insight and structure–activity relationships, we recently introduced the concept of "*Shim Chemistry*" [76], a catalyst design philosophy inspired by the adjustment of magnetic field homogeneity in NMR experiments, which provides a framework for systematic catalyst optimization. Guided by this approach, we have developed Rh–NHC-based successive generations of catalysts for efficient Markovnikov-selective alkyne hydrothiolation [77, 78] and alkyne dimerization [79–83]. In line with this strategy, we now report on the synthesis of a series of $[Rh(\mu\text{-}Cl)(\eta^2\text{-coe})(NHC)]_2$ complexes featuring NHC ligands with distinct stereoelectronic properties and evaluate their impact on the catalytic performance in alkyne hydropyridonation.

2 | Results and Discussion

2.1 | Synthesis of [Rh(μ-Cl)(η^2-Coe)(NHC)]$_2$ and RhCl(η^2-Coe)(NHC)(py) Complexes

Dinuclear complexes of type [Rh(μ-Cl)(η^2-coe)(NHC)]$_2$ (**2**-**4**) {NHC; IPr^{BIAN} = 1,3-bis(2,6-diisopropylphenyl)acenaphthoimidazolin-2-carbene (**2**); IPr^{Cl} = 1,3-bis(2,6-diisopropylphenyl)-4,5-dichloroimidazolin-2-carbene (**3**); IPr* = 1,3-bis{2,6-bis(diphenylmethyl)-4-methylphenyl}imidazolin-2-carbene (**4**)} were prepared from the organometallic precursor [Rh(μ-Cl)(η^2-coe)$_2$]$_2$ [84] via substitution of one olefin by the corresponding NHC at each rhodium center (Scheme 1). The stability of the free carbene dictates the synthetic strategy. Thus, in the case of **2**, the moderately unstable carbene IPr^{BIAN} [85] was generated in situ, whereas the isolated free carbenes IPr^{Cl} [86] or IPr* [87, 88] were used directly to obtain complexes **3** and **4**, respectively. The reactivity of the [Rh(μ-Cl)(η^2-coe)(NHC)]$_2$ framework imposes certain limitations on the nature of NHC ligands that can be incorporated. In particular, activation of the wingtip substituents has been reported for related systems [24–26, 29, 89, 90], and decreasing of the steric bulk of the NHC ligand often results in the undesired formation of bis- or tris-NHC rhodium complexes rather than the targeted dinuclear species [91–94]. Furthermore, formation of metal-peroxides [95–97] or paramagnetic Rh^{II} species [29, 95] may occur if strictly inert conditions are not maintained. In this regard, complex **4**, bearing the bulky IPr* ligand, undergoes partial decomposition during the work-up for isolation; therefore, in situ preparation in an NMR tube provides a more reliable synthetic method. Attempts to incorporate a more electron-rich ligand such as IPr^{Me} [98] {1,3-bis(2,6-diisopropylphenyl)-4,5-dimethylimidazolin-2-carbene}, less bulky derivatives, including IMe [99] (1,3-dimethylimidazolin-2-carbene), ICy [100] (1,3-dicyclohexylimidazolin-2-carbene), and IMeDipp {1-methyl-3-(2,6-diisopropylphenyl)imidazolin-2-carbene} [101], as well as difunctionalized scaffolds, IBuCou [102] [1-butyl-3-{(7,8-dimethyl-2H-coumarin-4-yl)methyl}imidazolin-2-carbene], IDippOpy [103] {1-(6-hydroxypyridin-2-yl)-3-(2,6-diisopropylphenyl)imidazolin-2-carbene}, IDippAmd [83] {1-(2-benzamidoethyl)-3-(2,6-diisopropylphenyl)imidazolin-2-carbene}, or IDippCarbx [104] {1-(2-carboxyethyl)-3-(2,6-diisopropylphenyl)imidazolin-2-carbene}, were unsuccessful.

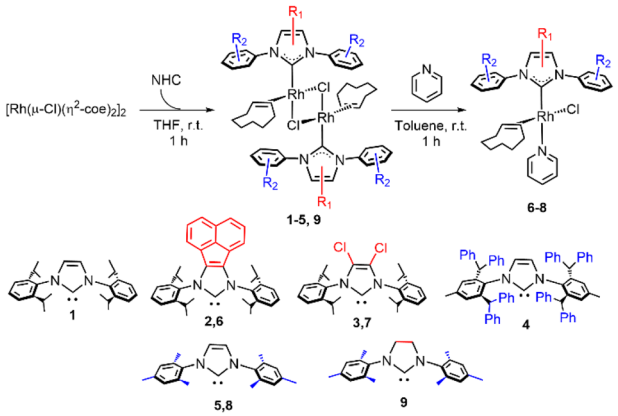

SCHEME 1 | Preparation of complexes **1–9**.

The solid-state structure of complexes **2** and **3** was determined by X-ray diffraction analysis on single crystals obtained by slow diffusion of *n*-hexane into concentrated CH_2Cl_2 solutions of **2** or slow evaporation of a C_6D_6 solution of **3** (Figure 1). The crystal structure in both cases shows a planar dinuclear chlorido-bridged Rh_2Cl_2 core with symmetry-related rhodium and chloro atoms. The coordination sphere of each metal center is completed by the NHC [**2**, C1-Rh 1.9512(17), **3**, C1-Rh 1.9488(13) Å] and coe ligands [**2**, Ct-Rh 1.976(2); **3**, Ct-Rh 1.986(2) Å] rendering a square planar environment and a trans disposition of the NHC and coe ligands at the dinuclear core, respectively. The intermetallic distance Rh···Rh' [**2**, 3.7389(1); **3**, 3.7469(4) Å] rules out any metal–metal interaction. The NHC ring C1-N2-C3-C4-N5 lies almost perpendicular to the coordination plane [**2**, N2-C1-Rh-Cl1 92.2(1); **3**, N5-C1-Rh-Cl1 90.7(1)°] and tilts away from the adjacent coe ligand [pitch angles θ 11.8° (**2**) and 11.6° (**3**)],

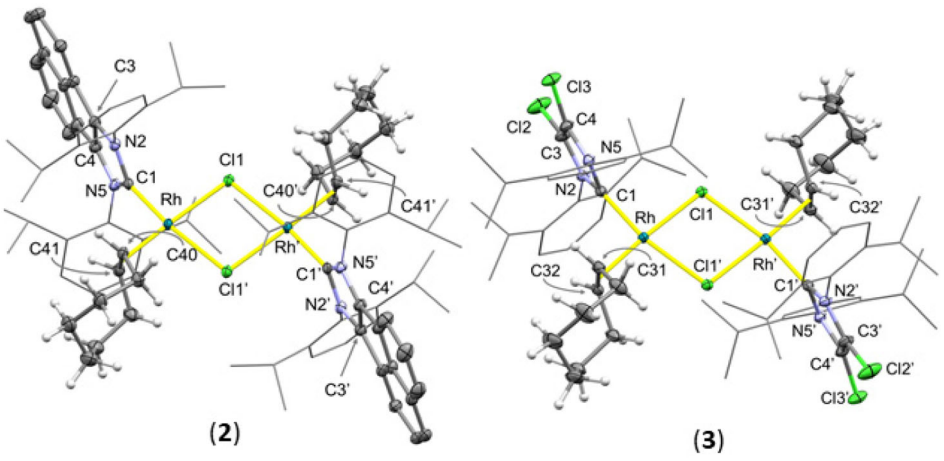

FIGURE 1 | ORTEP views of **2** and **3**. Ellipsoids are at 50% probability, and most hydrogen atoms have been omitted for clarity. Selected bond lengths (Å) and angles (°) are: **2**, C1-Rh 1.9512(17), Cl1-Rh 2.4229(4), Rh-Cl1' 2.4630(4), Ct-Rh 1.976(2), C41-Rh 2.1070(17), C40-Rh 2.0933(18), C41-C42 1.509(3), C1-Rh-Cl1' 169.76(5), Cl1-Rh-Cl1' 80.146(15), C1-Rh-Cl1 91.15(5), Ct-Rh-C1 92.33(7), Rh-Cl-Rh' 99.854(15), pitch θ 11.8, yaw ψ 2.3, Ct centroid of C41 and C42; **3**, C1-Rh 1.9488(13), Cl1-Rh 2.4209(3), Rh-Cl1' 2.4662(3), Ct-Rh 1.986(2), C31-C32 1.403(2), C31-Rh 2.1120(14), C32-Rh 2.1027(14), C1-Rh-Cl' 90.62(4), C1-Rh-Cl1 168.90(4), Cl1'-Rh-Cl1 79.888(12), Ct-Rh-C1 92.82(6), Rh'-Cl1-Rh 100.113(12), pitch θ 11.6, yaw ψ 3.1, Ct centroid of C31 and C32. Symmetry operation for equivalent atoms: $-x+2$, $-y$, $-z+1$.

reasonably as a consequence of the steric congestion between coe and the NHC wingtips. Also, due to the higher trans influence of the carbene ligands when compared with coe, the rhodium–chloro bond length Rh-Cl1' is longer than Rh-Cl1 [**2** Cl1-Rh 2.4229(4), Rh-Cl1' 2.4630(4); **3**, Cl1-Rh 2.4209(3), Rh-Cl1' 2.4662(3) Å].

An interesting feature emerges from the analysis of the intermolecular interactions in the crystal structure of complex **3**. A symmetrical type I halogen bond is observed between the chlorine atoms of the functionalized NHC ligand, as indicated by the Cl3···Cl3″ separation of 3.197 Å and the C3–Cl3···Cl3″ angle of 160.6° (Figure 2) [105–107]. These noncovalent Cl···Cl contacts give rise to one-dimensional chains extending parallel to the $\vec{c}-\vec{a}$ direction. Although halogen bonding between the lone pair of an NHC as an electron donor and the σ-hole of a chloride atom has been explored computationally [107], to the best of our knowledge, no Cl···Cl halogen bond involving the chlorinated NHC ligand IPr^{Cl} has been previously described.

The NMR spectroscopic data of complexes **2–4** confirm that the solid-state structure is maintained in solution. The ^{1}H NMR spectra of complexes **2** and **3** recorded at room temperature exhibit broadened resonances for the isopropyl substituents, a feature commonly attributed to restricted rotation of the NHC ligand about the Rh—C bond on the NMR timescale [31, 97]. This fluxional process is frozen out at −20°C. At this temperature, the characteristic resonances of both the η^2-coe and the corresponding NHC ligand are observed in the ^{1}H and $^{13}C\{^{1}H\}$-APT NMR spectra. The chemical shift of the carbene carbon atom varies significantly among the different NHC ligands, appearing at δ 191.9 ppm for IPr^{BIAN}, 185.6 ppm for IPr^{Cl}, and 177.0 ppm for IPr*. Particularly for the IPr* counterpart, an inversion of the chemical shifts between the wingtip aliphatic protons (δ 6.40 ppm) and the imidazolium backbone ones (δ 4.58 ppm) is observed, a feature typically found in these derivatives [108–113].

The chlorido-bridge of dinuclear species [Rh(μ-Cl)(η^2-olefin)(NHC)]$_2$ can be cleaved upon addition of nucleophilic ligands [31, 36]. Thus, treatment of **2**, **3**, and [Rh(μ-Cl)(η^2-coe)(IMes)]$_2$ (**5**) [26] with pyridine (py) in toluene for 1 hr at room temperature resulted in the formation of mononuclear RhCl(η^2-coe)(NHC)(py) **6–8** derivatives {NHC = IPr^{BIAN} (**6**), IPr^{Cl} (**7**), IMes (**8**)}, which were isolated as yellow solids in 62%–79% yields (Scheme 1). A mutually trans NHC-py disposition is assumed based on previously reported analogous complexes characterized by X-ray analysis [31, 97]. The most noticeable feature of the NMR spectra is the presence of pyridine signals without loss of the diagnostic resonances of the η^2-coe and NHC ligands. Unlike dinuclear complexes **2–3**, the pyridine derivatives exhibit well-resolved isopropyl resonances at room temperature, consistent with an increased energy barrier for the rhodium-carbene rotational process. In addition, the carbene carbon doublets of Rh-py derivatives in the $^{13}C\{^{1}H\}$-APT NMR spectra are deshielded by approximately 4 ppm, accompanied by a decrease of the $J_{C\text{-}Rh}$ value by around 8 Hz, indicating increased electron density at the rhodium center in complexes **6–8** [114].

2.2 | Catalytic Activity in Alkyne Hydropyridonation

We have previously communicated that the dinuclear complex [Rh(μ-Cl)(η^2-coe)(IPr)]$_2$ (**1**) is an efficient catalyst for alkyne hydropyridonation, selectively affording *O-gem*-alkenyl-oxypyridines (Scheme 2) [75]. The proposed mechanism begins with coordination of both the pyridone and the alkyne ligands, enabled by chlorido-bridge cleavage and η^2-coe decoordination from the dinuclear Rh–NHC precatalyst. Subsequently, an intramolecular oxidative protonation of a π-alkyne at its terminal carbon by a k^1N-bound hydroxypyridine ligand accounts for the *gem*-specificity observed in the catalytic outcome. At this stage, since direct reductive elimination within the resulting alkenyl-pyridonato intermediate was found to be energetically inaccessible, isomerization to a metalacyclopropene species provides an alternative pathway that enables the subsequent nucleophilic attack. The chemoselectivity formation of the less thermodynamically favored *O*-alkenylated products most likely arises from the preferred coordination of a pyridine moiety *trans* to NHC, which induces a seesaw effect responsible of the *O*-nucleophilic attack. Finally, the release of the coupled product regenerates the catalytically active species, which has been identified as the rate-determining step of the overall process.

The catalytic activity of the newly prepared NHC-functionalized rhodium complexes **2–4** and **8**, as well as the previously reported derivatives [Rh(μ-Cl)(η^2-coe)(IMes)]$_2$ (**5**) {IMes = 1,3-bis(2,4,6-trimethylphenyl)imidazolin-2-carbene}, and [Rh(μ-Cl)(η^2-coe)(SIMes)]$_2$ (**9**) {SIMes = 1,3-bis(2,4,6-trimethylphenyl)imidazolidin-2-carbene} has been evaluated. The addition of 2-pyridone to phenylacetylene (1:1 ratio) was chosen as a benchmark reaction. Catalytic experiments were carried out in NMR

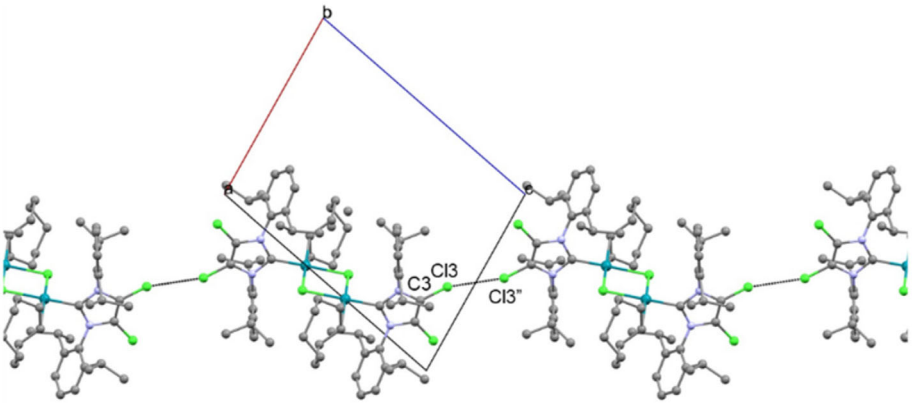

FIGURE 2 | View of the Cl···Cl intermolecular contacts in **3** and the resulting 1D chain. Symmetry operation for equivalent atoms: −2x + 2, −y, +1.

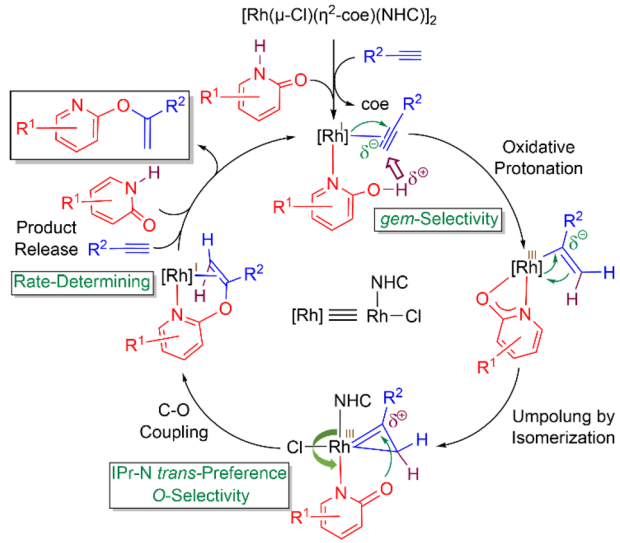

SCHEME 2 | Mechanistic proposal for alkyne hydropyridonation.

tubes in $CDCl_3$ (0.5 mL) using 5 mol% of catalyst loading at 50°C directly inside the NMR spectrometer. The reaction progress was monitored through sequential ^{1}H NMR spectra acquired at regular time intervals, enabling the operando direct observation of substrate consumption and product formation (Figure 3, Table 1). This setup provided reproducible kinetic profiles suitable for comparative evaluation of catalyst performance.

Several studies have reported superior catalytic performance of IPr^{BIAN}-based complexes compared to their IPr analogs [115–118], a trend generally attributed to their greater robustness and stronger σ-donating ability [119–121], although examples of reduced activity have also been documented [122]. Notably, the enhanced stability of the Rh–IPr^{BIAN} bond was anticipated to be a key factor in improving catalytic efficiency, as decomposition to the corresponding imidazolium salt in protic media [123] has been identified as a major limitation of this catalytic system [75]. Despite this, the catalytic performance of Rh–IPr^{BIAN} catalyst **2** in alkyne hydropyridonation is lower than that of the Rh–IPr complex **1**, achieving only 45% conversion after

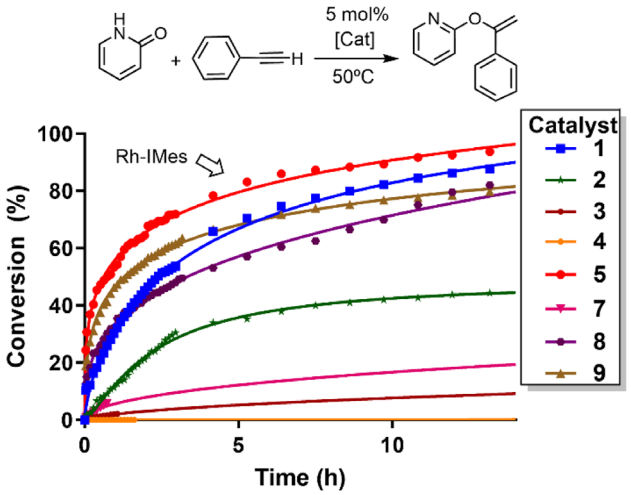

FIGURE 3 | Reaction profile for the hydropyridonation of phenylacetylene with 2-pyridone for different Rh–NHC catalysts.

TABLE 1 | Catalyst screening for the hydropyridonation of phenylacetylene with 2-pyridone[a].

Entry	Cat.	Conv., %[b]	*Gem*-dimer	*O*-alkenyl-oxypyridine	*N*-alkenyl-pyridone
1	**1**	88	5	95	—
2	**2**	45	—	>99	—
3	**3**	9	—	>99	—
4	**4**	<1	—		—
5	**5**	95	—	>99	—
6	**7**	19	23	77	—
7	**8**	84	1	99	—
8	**9**	81	—	>99	—

[a]Reaction conditions: 0.20 mmol of phenylacetylene, 0.20 mmol of 2-pyridone, 0.07 mmol of mesitylene (internal standard), 5 mol% catalyst based on Rh atom (2.5 mol% for dinuclear complexes), 0.5 mL of $CDCl_3$, 50°C, 14 h.
[b]Conversion of phenylacetylene.

14 h at 50°C (entry 2). Alternatively, decreasing the electron-donating ability of the NHC by introducing the IPr^{Cl} ligand [124] in catalyst **3** led to an even lower conversion (9%, entry 3). Conversely, increasing the steric bulk at the carbene wingtip in the IPr* catalyst **4** almost completely inhibited catalytic activity (entry 4). Nevertheless, replacing the IPr ligand with IMes in catalyst **5** gratifyingly led to enhanced catalytic performance (entry 5). Not only does the conversion after 14 h increased to 95%, but the selectivity toward the *O*-alkenylated derivative also rises up to 99%. In view of this, further modifications of the Rh–IMes framework were investigated. However, the mononuclear IMes-pyridine catalyst **8** is slightly less active than **5**, affording 84% conversion (entry 7). In addition, incorporation of the saturated SIMes ligand in complex **9** also leads to a slight decrease in catalytic efficiency compared to complex **5** (entry 8 Cross-Coupling Reactions Of Organoboranes: An Easy Way To Construct C-C Bonds (Nobel Lecture)). It is worth noting the excellent selectivity for the *O*-alkenylated product achieved with both catalysts (>99%).

The catalytic performance of the most active catalyst of the series, complex **5**, was further evaluated using various combinations of pyridone and alkyne substrates (Figure 4). The aliphatic cyclopropylacetylene substrate exhibited lower reactivity than phenylacetylene with catalyst **1**, affording only 72% conversion before catalyst decomposition occurred. The trend in alkyne reactivity was maintained for catalyst **5**. However, complete conversion and high selectivity toward a single *O*-alkenylated product were achieved. In other way, 6-chloro-2-pyridone represents a particular case, as the formation of the *N*-alkenylated product was also observed with catalyst **1**, resulting in an *O*- to *N*-selectivity ratio of 53:30, along with formation of 17% of *gem*-dimers [75]. Under similar conditions, catalyst **5** afforded 85% selectivity for the *O*-alkenylated product, suppressing the formation of alkyne dimers. Interesting to point out is that differentiating between potential *O*- or *N*-alkenylated products is challenging based solely on ^{13}C NMR data, as the chemical shift of the C2-imidic (C–O coupling) and C2-amidic (C–N coupling) carbon atoms differ only slightly. At this point, the 2D ^{1}H-^{15}N NMR experiment proved crucial for an unambiguous characterization, as a correlation between one olefinic proton and the nitrogen atom is observed for the

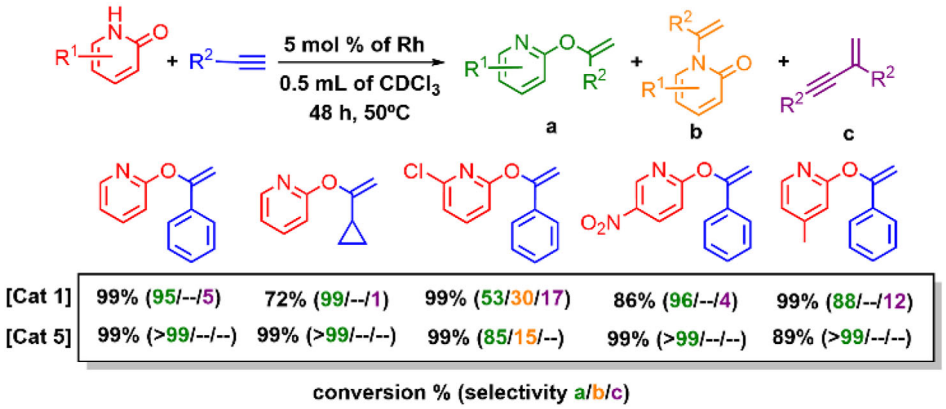

FIGURE 4 | Comparison of catalytic activity of **1** and **5** for different substrates.

N-alkenylated product, whereas it is absent in the *O*-alkenylated counterpart, in which the two nuclei are five bonds away. Moreover, catalyst **5** is also more active in the transformation of 5-nitro-2-pyridone. However, its activity for 4-methyl-2-pyridone is lower, although the reaction proceeds with higher selectivity for hydropyridonation.

Rh–NHC dinuclear catalysts efficiently promote alkyne hydropyridonation, with both steric and electronic effects exerting a decisive influence on activity and selectivity. While a comprehensive assessment of various NHC ligands is limited by the challenging synthesis of Rh–NHC dinuclear species, distinct structure–reactivity trends can nevertheless be discerned from the present study. Taking the IPr ligand as a reference, reducing its σ-donation in IPr^{Cl} proves detrimental to catalytic activity, as a more electron-poor rhodium center should disfavor both μ-Cl bridge cleavage and the oxidative protonation step. Moreover, the highly hindered metal environment provided by IPr* completely suppresses catalysis, most likely because steric crowding around rhodium prevents the simultaneous coordination of alkyne and pyridone ligands required for productive turnover. At this point, it is important to note that introducing a chloro substituent on the imidazole backbone also increases steric hindrance due to a buttressing effect. In contrast, the IMes complex displays the highest reactivity in the series, suggesting that moderate steric demand combined with balanced σ-donation facilitates precatalyst activation and substrate exchange. The reduced activity of IPr^{BIAN}, despite its stronger donor character, can therefore be attributed to its rigid, axially encumbered framework, which hampers access to adjacent coordination sites. Overall, catalytic performance appears to be governed not by the electronic strength of the carbene alone but by the way each NHC modulates the dynamic lability of the metal environment. Within this window, IMes achieves the optimal compromise between stability and reactivity, while both overly donating or excessively hindered ligands deactivate the system. Smaller NHCs, such as IMe, ICy, or IMeDipp, could, in principle, further enhance turnover. However, attempts to isolate the corresponding Rh–NHC dinuclear complexes have so far been unsuccessful, preventing experimental verification of this hypothesis.

3 | Conclusion

A series of new Rh^{I}–NHC dinuclear complexes of type [Rh(μ-Cl)(η^2-coe)(NHC)]$_2$, containing IPr^{BIAN}, IPr^{Cl}, and IPr* ligands, has been prepared and characterized by NMR spectroscopy, with single-crystal X-ray diffraction for the first two complexes. Notably, a symmetrical type I noncovalent halogen bond has been observed between the chlorine atoms of the functionalized NHC ligand in the crystal structure of the IPr^{Cl} dinuclear complex. The chlorido-bridges can be cleaved by pyridine to afford the mononuclear derivatives RhCl(η^2-coe)(NHC)(py). The catalytic activity for alkyne hydropyridonation has been studied, revealing that both steric and electronic effects exert a decisive influence. Taking the IPr ligand as a reference, a reduction of its σ-donation (IPr^{Cl}) or an increment in the steric hindrance by (IPr*) proved detrimental to the catalytic performance. In contrast, the IMes complex displays the highest reactivity of the series, suggesting that a moderate steric demand combined with balanced σ-donation facilitates precatalyst activation and substrate exchange. Further studies are currently underway in our laboratories to develop more efficient alkyne pyridonation catalysts incorporating alternative NHC motifs.

4 | Experimental Section

4.1 | General Considerations

All reactions were carried out with rigorous exclusion of air and moisture using Schlenk-tube techniques and a dry box when necessary. Reagents were purchased from commercial suppliers and used as received, except for phenylacetylene, which was first dried over molecular sieves and then distilled and stored over anhydrous $CaCl_2$. Organic solvents were obtained oxygen- and water-free from a Solvent Purification System (Innovative Technologies). Deuterated solvents were dried and deoxygenated prior to use: C_6D_6, toluene-d_8, and THF-d_8 with sodium, CD_2Cl_2 with calcium hydride, and $CDCl_3$ with molecular sieves. The organometallic precursors [Rh(μ-Cl)(η^2-coe)$_2$]$_2$ [84], [Rh(μ-Cl)(η^2-coe)(IPr)]$_2$ (**1**) [26], and [Rh(μ-Cl)(η^2-coe)(IMes)]$_2$ (**5**) [26], and carbenes IPr^{BIAN} [85], IPr^{Cl} [86], and IPr* [87, 88] were prepared as previously described in the literature. NMR spectra were recorded on either a Bruker ARX 300 MHz, a Bruker Avance 400 MHz, or a Bruker Avance 500 MHz instrument. NMR chemical shifts (expressed in parts per million) are referenced to residual solvent peaks (^{1}H and ^{13}C). Coupling constants, *J*, are given in hertz (Hz). Spectral assignments were achieved by combination of ^{1}H, ^{13}C{^{1}H}-APT, ^{1}H-^{1}H COSY, and ^{1}H-^{13}C HSQC and HMBC experiments. C, H, and N analyses were

carried out in a Perkin-Elmer 2400 CHNS/O analyzer. High-resolution electrospray ionization mass spectra (HRMS-ESI) were recorded using a Bruker MicroToF-Q equipped with an API-ESI source and a Q-ToF mass analyzer, which leads to a maximum error in the measurement of 5 ppm, using sodium formate as a reference.

4.2 | Preparation of $[Rh(\mu\text{-}Cl)(\eta^2\text{-}coe)(IPr^{BIAN})]_2$ (2)

A mixture of $[HIPr^{BIAN}]Cl$ (336 mg, 0.60 mmol) and KO^{t}Bu (76 mg, 0.65 mmol) in 20 mL of THF was stirred for 30 min at r.t. Then, a solution of $[Rh(\mu\text{-}Cl)(\eta^2\text{-}coe)_2]_2$ (200 mg, 0.28 mmol) in 10 mL of THF was cannulated to this mixture and was stirred for 1 h at r.t. After removal of the solvent, the residue was dissolved in toluene (15 mL), and it was filtered through celite. The filtrate was evaporated to dryness and the addition of *n*-hexane induced the precipitation of a yellow solid, which was washed with *n*-hexane (3 × 4 mL) and dried in vacuo. Yield: 182 mg (42%). HRMS (ESI+): m/z Calcd for $C_{74}H_{80}Cl_2N_4Rh_2$ $[M\text{-}2coe]^+$: 1300.3864. Exp: 1300.3852. ^{1}H NMR (400 MHz, THF-d_8, 243 K): δ 7.7–7.3 (m, 12H, H_{Ph}), 7.57 (d, J_{H-H} = 8.3, 4H, $H_{5\text{-}BIAN}$), 7.21 (t, J_{H-H} = 8.3, 7,7, 4H, $H_{4\text{-}BIAN}$), 6.70 (d, J_{H-H} = 7.7, 4H, $H_{3\text{-}BIAN}$), 4.00 and 2.30 (both sept, J_{H-H} = 6.1, 8H, C<u>H</u>Me), 2.86 (br, 2H, =CH_{coe}), 1.6–0.8(m, 12H, $CH_{2\text{-}coe}$), 1.59, 1.28, 1.09, and 0.69 (all d, J_{H-H} = 6.1, 48H, Me). $^{13}C\{^1H\}$-APT NMR (100.5 MHz, THF-d_8, 243 K): 191.9 (d, $J_{C\text{-}Rh}$ = 61.4, Rh-C_{BIAN}), 148.6 and 147.9 ($C_{q\text{-}Ph}$), 141.0 ($C_{1\text{-}BIAN}$), 137.1 (C_qN_{Ph}), 130.8, 125.4, and 125.0 (CH_{Ph}), 130.8 ($C_{2a\text{-}BIAN}$), 130.2 ($C_{2b\text{-}BIAN}$), 128.2 (C_5H_{BIAN}), 127.9 (C_4H_{BIAN}), 127.8 ($C_{5a\text{-}BIAN}$), 122.0 (C_3H_{BIAN}), 57.0 (d, $J_{C\text{-}Rh}$ = 17.0, =CH_{coe}), 30.8, 30.2, and 27.1 ($CH_{2\text{-}coe}$), 29.4 and 28.6 (<u>C</u>HMe), 25.5, 25,0, 24.9, and 23.2 (Me).

4.3 | Preparation of $[Rh(\mu\text{-}Cl)(\eta^2\text{-}coe)(IPr^{Cl})]_2$ (3)

A mixture of $[Rh(\mu\text{-}Cl)(\eta^2\text{-}coe)_2]_2$ (294 mg, 0.41 mmol) and IPr^{Cl} (366 mg, 0.80 mmol) in 20 mL of THF was stirred for 1 h at r.t. After removal of the solvent, the residue was dissolved in toluene (15 mL), and it was filtered through celite. Then, the filtrate was evaporated to dryness. The addition of *n*-hexane induced the precipitation of a yellow solid, which was washed with *n*-hexane (3 × 4 mL) and dried in vacuo. Yield: 454 mg (81%). Anal. calcd for $C_{70}H_{96}N_4Cl_6Rh_2$: C, 59.54; H, 6.85; N, 3.97. Found: C, 59.45; H, 7.13; N, 4.13. ^{1}H NMR (400 MHz, toluene-d_8, 253 K): δ 7.6–7.0 (12H, H_{Ph}), 3.79 and 2.13 (both sept, J_{H-H} = 6.6, 8H, C<u>H</u>Me), 2.91 (m, 4H, =CH_{coe}), 2.1–1.2 (24H, $CH_{2\text{-}coe}$), 1.60, 1.30, 1.12, and 1.05 (all d, J_{H-H} = 6.6, 48H, Me). $^{13}C\{^1H\}$-APT NMR (100 MHz, toluene-d_8, 253 K): δ 185.6 (d, $J_{C\text{-}Rh}$ = 63.7, Rh-C_{NHC}), 148.9 and 146.5 ($C_{q\text{-}NHC}$), 134.0 (C_qN), 130.5 ($CH_{p\text{-}Ph}$), 125.8 and 123.7 ($CH_{m\text{-}Ph\text{-}}$), 118.2 (=CClN), 57.0 (d, $J_{C\text{-}Rh}$ = 16.6 =CH_{coe}), 30.1, 30.0, and 27.1 ($CH_{2\text{-}coe}$), 28.8 and 28.7 (<u>C</u>HMe), 26.2, 26.1, 25.1, and 23.9 (Me).

4.4 | *In situ* formation of $[Rh(\mu\text{-}Cl)(\eta^2\text{-}coe)(IPr^*)]_2$ (4)

This complex was prepared from $[Rh(\mu\text{-}Cl)(\eta^2\text{-}coe)_2]_2$ (8.2 mg, 0.02 mmol) and IPr* (20 mg, 0.04 mmol) in THF-d_8 at 298K (0.5 mL, NMR tube). HRMS (ESI+): m/z Calcd for $C_{138}H_{112}Cl_2N_4Rh$: $[M\text{-}2coe]^+$: 2100.6368. Exp: 2100.6358.^{1}H NMR (400 MHz, THF-d_8, 298K): 7.5–6.6 (m, 88H, H_{Ph}), 6.40 (s, 8H, C<u>H</u>Ph_2), 4.58 (s, 4H, =CHN), 3.23 (m, 4H, =CH_{coe}), 2.22 (s, 12H, Me), 1.6–1.2 (m, 24H, $CH_{2\text{-}coe}$). $^{13}C\{^1H\}$-APT NMR (100.5 MHz, THF-d_8, 298 K): δ 177.0 (d, $J_{C\text{-}Rh}$ = 64.8, Rh-C_{IPr^*}), 146.0 and 145.5 ($C_{q\text{-}Ph}$), 144.2 ($C_{q\text{-}CHPh}$), 138.4 ($C_{q\text{-}MePh}$), 138.2 (C_qN), 131.9, 130.7, 130.6, 128.8, 128.6, and 126.9 (CH_{Ph}), 124.2 (=CHN), 60.4 (d, $J_{C\text{-}Rh}$ = 16.0, =CH_{coe}), 52.3 (s, <u>C</u>HPh_2), 30.8, 30.2, and 27.2 (all s, $CH_{2\text{-}coe}$), 21.8 (s, Me_{Ph}).

4.5 | Preparation of $RhCl(\eta^2\text{-}coe)(IPr^{BIAN})(py)$ (6)

A solution of **2** (133 mg, 0.08 mmol) in toluene (15 mL) was treated with pyridine (20 µL, 0.24 mmol), and it was stirred for 1 h at r.t. Then, the solution was filtered through celite, and the filtrate was evaporated to dryness. The addition of *n*-hexane induced the precipitation of a yellow solid, which was washed with *n*-hexane (3 × 4 mL) and dried in vacuo. Yield: 83 mg (62%). Anal. calcd for $C_{50}H_{59}ClN_3Rh$: C, 71.46; H, 7.08; N, 5.00. Found: C, 71.23; H, 6.69; N, 4.96. ^{1}H NMR (400 MHz, toluene-d_8, 253K): δ 8.44 (d, J_{H-H} = 5.2, 2H, $H_{2\text{-}py}$), 7.58 (dd, J_{H-H} = 7.7, 1.5, 2H, $H_{p\text{-}Ph}$), 7.50 (t, J_{H-H} = 7.7, 2H, $H_{m\text{-}Ph}$), 7.27 (dd, J_{H-H} = 7.7, 1.5, 2H, $H_{m\text{-}Ph}$), 7.17 (dd, J_{H-H} = 5.2, 3.9, 2H, $H_{4\text{-}BIAN}$), 6.81 (m, 4H, $H_{3,5\text{-}BIAN}$), 6.56 (t, J_{H-H} = 7.8, 1H, $H_{4\text{-}py}$), 6.25 (dd, J_{H-H} = 7.8, 5.2, 2H, $H_{3\text{-}py}$), 4.98 and 2.70 (sept, J_{H-H} = 6.6, 4H, C<u>H</u>Me), 3.41 (m, 2H, =CH_{coe}), 1.7 – 0.8 (m, 12H, $CH_{2\text{-}coe}$), 1.85, 1.43, 1.16, and 0.86 (all d, J_{H-H} = 6.6, 24H, Me). $^{13}C\{^1H\}$-APT NMR (100.5 MHz, Toluene-d_8, 253 K): 195.4 (d, $J_{C\text{-}Rh}$ = 54.3, Rh-C_{BIAN}), 153.3 ($C_{2\text{-}py}$), 149.5 and 146.2 ($C_{q\text{-}Ph}$), 140.2 ($C_{1\text{-}BIAN}$), 136.4 (C_qN_{Ph}), 134.8 (C_4H_{py}), 130.3 ($CH_{p\text{-}Ph}$), 129.9 and 129.8 ($C_{2a,\ 2b\text{-}BIAN}$), 128.6 ($C_{5a\text{-}BIAN}$), 127.3 (C_4H_{BIAN}), 127.1 (C_5H_{BIAN}), 125.7 and 123.4 ($CH_{m\text{-}Ph}$), 122.5 (s, C_3H_{py}), 121.5 (C_3H_{BIAN}), 55.3 (d, $J_{C\text{-}Rh}$ = 16.7, =CH_{coe}), 29.2 and 29.1 (<u>C</u>HMe), 32.1, 29.7, 29.5, 26.7, 26.3, and 25.6 ($CH_{2\text{-}coe}$), 26.1, 25.9, 25.6, and 23.4 (Me).

4.6 | Preparation of $RhCl(\eta^2\text{-}coe)(IPr^{Cl})(py)$ (7)

This compound was prepared as described for **6** starting from **3** (125 mg, 0.09 mmol) and pyridine (20 µL, 0.24 mmol). Yellow solid. Yield: 125 mg (79%). Anal. calcd for $C_{40}H_{53}N_3Cl_3Rh$: C, 61.19; H, 6.80; N, 5.35. Found: C, 60.95; H, 7.17; N, 5.48. ^{1}H NMR (300 MHz, C_6D_6, 298 K): δ 8.35 (d, J_{H-H} = 5.0, 2H, $H_{2\text{-}py}$), 7.46 and 7.16 (both m, 4H, $H_{m\text{-}Ph}$), 7.37 (t, 2H, $H_{o\text{-}Ph}$), 6.52 (d, J_{H-H} = 7.5, 1H, $H_{4\text{-}py}$), 6.21 (dd, J_{H-H} = 7.3, 5.0, 2H, $H_{3\text{-}py}$), 4.54 and 2.39 (both sept, J_{H-H} = 6.6, 4H, C<u>H</u>Me_{IPrCl}), 3.21 (m, 2H, =CH_{coe}), 1.8–0.9 (12H, $CH_{2\text{-}coe}$), 1.82, 1.39, 1.24, and 1.11 (all d, J_{H-H} = 6.6, 24H, Me_{IPrCl}). $^{13}C\{^1H\}$-APT NMR (75 MHz, C_6D_6, 298 K): δ 190.7 (d, $J_{C\text{-}Rh}$ = 54.5, Rh-C_{IPrCl}), 153.3 (C_2H_{py}), 150.5 and 146.9 ($C_{q\text{-}IPrCl}$), 135.0 (C_4H_{py}), 134.8 (C_qN), 130.7 ($CH_{p\text{-}Ph\text{-}IPrCl}$), 126.1 and 123.4 ($CH_{m\text{-}Ph\text{-}IPrCl}$), 122.6 ($C_3H_{py}$), 118.8 (=CClN), 56.3 (d, $J_{C\text{-}Rh}$ = 15.5 =CH_{coe}), 30.1, (d, $J_{C\text{-}Rh}$ = 1.5 $CH_{2\text{-}coe}$), 29.8, and 26.9 ($CH_{2\text{-}coe}$), 29.3 and 29.1 (<u>C</u>HMe), 26.6, 25.9, 25.6, and 23.9 (Me).

4.7 | Preparation of $RhCl(\eta^2\text{-}coe)(IMes)(py)$ (8)

This compound was prepared as described for **6** starting from **5** (155 mg, 0.14 mmol) and pyridine (34 µL, 0.42 mmol). Yellow solid. Yield: 110 mg (62%). HRMS (ESI+): m/z Calcd for $C_{34}H_{43}ClN_3Rh$: $[M\text{-}C_8H_{14}\text{-}Cl]^+$: 486.1411. Exp: 486.1405. ^{1}H NMR (300 MHz, C_6D_6, 298 K): δ 8.38 (d, J_{H-H} = 4.0, 2H,

$H_{2\text{-Py}}$), 6.94 and 6.90 (both s, 4H, $H_{3\text{-IMes}}$), 6.52 (t, $J_{H-H} = 6.8$, 1H, $H_{4\text{-Py}}$), 6.21 (s, 2H, =CHN), 6.15 (t, $J_{H-H} = 5.8$, 2H, $H_{3\text{-Py}}$), 3.13 (m, 2H, $=CH_{coe}$), 2.80 and 2.24 (s, 6H, $Me_{o\text{-IMes}}$), 2.19 (both s, 12H, $Me_{p\text{-IMes}}$), 1.8–1.1 (12H, $CH_{2\text{-coe}}$). $^{13}C\{^1H\}$-APT NMR (75 MHz, C_6D_6, 298 K): δ 183.7 (d, $J_{C\text{-Rh}} = 53.4$, Rh-C_{IMes}), 153.6 (C_2H_{py}), 139.0 and 135.0 ($C_{q\text{-o-IMes}}$), 138.1 ($C_{q\text{-p-IMes}}$), 137.9 (C_qN_{IMes}), 134.7 (C_4H_{Py}), 130.3 and 128.2 ($CH_{m\text{-IMes}}$), 123.2 (=CHN), 122.4 (C_3H_{Py}), 55.5 (d, $J_{C\text{-Rh}} = 16.7$, $=CH_{coe}$), 30.6, 29.8, and 27.1 ($CH_{2\text{-coe}}$), 21.2 and 18.5 ($Me_{o\text{-IMes}}$), 20.8 ($Me_{p\text{-IMes}}$).

4.8 | Standard Conditions for the Catalytic Reactions

Alkyne hydropyridonation catalytic reactions were carried out in NMR tubes under argon atmosphere. In a typical experiment, an NMR tube was charged with the catalyst (5 mol% based on Rh atom, 0.01 mmol), alkyne (0.20 mmol), pyridone (0.20 mmol), mesitylene (0.07 mmol, internal standard), and $CDCl_3$ (0.5 mL). The sealed tube was placed in the NMR spectrometer and maintained at 50°C, and the reaction progress was monitored by ^1H NMR spectroscopy for the determined time. The reaction products were unambiguously characterized on the basis of NMR literature data [75]. Conversion and selectivities were determined by ^1H NMR spectroscopy.

4.9 | Crystal Structure Determination

Single crystals suitable for the X-ray diffraction studies were grown by slow diffusion of *n*-hexane over saturated CH_2Cl_2 solution of **2** or slow evaporation of C_6D_6 solution of **3**. X-ray diffraction data were collected at 100(2) K on a Venture D8 (**2**) or APEX DUO Bruker (**3**) diffractometer with graphite-monochromated Mo–Kα radiation ($\lambda = 0.71073$ Å) using ω-scans. Intensities were integrated and corrected for absorption effects with SAINT–PLUS [125] and SADABS [126] programs, both included in APEX4 package. The structures were solved by the Patterson method with SHELXS-97 [127] and refined by full matrix least-squares on F^2 with SHELXL-2014 [128] under WinGX [129]. Pitch and yaw angles have been calculated according to the literature [130].

4.10 | Crystal Data and Structure Refinement for 2

$C_{93}H_{114}Cl_8N_4Rh_2$, 1777.30 g mol^{-1}, triclinic, *P*–1, $a = 12.0571(5)$ Å, $b = 13.4056(7)$ Å, $c = 15.0626(7)$ Å, $\alpha = 89.508(2)°$, $\beta = 67.959(2)°$, $\gamma = 71.716(2)°$, $V = 2126.20(18)$ Å^3, $Z = 1$, $D_{calc} = 1.388$ g cm^{-3}, $\mu = 0.688$ mm^{-1}, $F(000) = 926$, $0.300 \times 0.290 \times 0.190$ mm^3, $\theta_{min}/\theta_{max}$ 1.934/28.338°, index ranges $-16 \le h \le 16$, $-17 \le k \le 17$, $-20 \le l \le 20$, reflections collected/independent 117 310/10 567 [R(int) = 0.0468], T_{max}/T_{min} 0.7457/0.6870, data/restraints/parameters 10 567/0/495, GooF(F^2) = 1.071, $R_1 = 0.0339$ [$I > 2\sigma$(I)], $wR_2 = 0.0887$ (all data), largest diff. peak/hole 1.736/–1.006 e Å^{-3}. CCDC deposit number 2 502 428.

4.11 | Crystal Data and Structure Refinement for 3

$C_{82}H_{108}Cl_6N_4Rh_2$, 1568.24 g mol^{-1}, triclinic, *P*–1, $a = 11.9432(4)$ Å, $b = 11.9671(4)$ Å, $c = 15.0437(5)$ Å, $\alpha = 81.55°$, $\beta = 76.20°$, $\gamma = 69.62°$, $V = 1952.50(11)$ Å^3, $Z = 1$, $D_{calc} = 1.334$ g cm^{-3}, $\mu = 0.673$ mm^{-1}, $F(000) = 820$, $0.200 \times 0.180 \times 0.80$ mm^3, $\theta_{min}/\theta_{max}$ 1.397/29.603°, index ranges $-16 \le h \le 16$, $-16 \le k \le 16$, $-20 \le l \le 20$, reflections collected/independent 41 351/10 275 [R(int) = 0.0293], T_{max}/T_{min} 0.8892/0.8129, data/restraints/parameters 10 275/3/459, GooF(F^2) = 1.054, $R_1 = 0.0251$ [$I > 2\sigma$ (I)], $wR_2 = 0.0644$ (all data), largest diff. peak/hole 0.605/–0.498 e Å^{-3}. CCDC deposit number 2 502 427.

Acknowledgments

Financial support from the Spanish Ministerio de Ciencia, Innovación y Universidades MICIU/AEI/10.13039/501100011033, under the Project PID2022-137208NB-I00, and the Departamento de Ciencia, Universidad y Sociedad del Conocimiento del Gobierno de Aragón (group E42_23R) is gratefully acknowledged. M.O.K. thankfully acknowledge the University of Zaragoza for a contract under the program "Unprotected Researchers". The use of the Servicio General de Apoyo a la Investigación-SAI of the University of Zaragoza, and the scientific-technical services of the ISQCH/CEQMA (CSIC) is gratefully acknowledged.

Funding

This study was supported by Ministerio de Ciencia, Innovación y Universidades (PID2022-137208NB-I00) and Departamento de Educación, Cultura y Deporte, Gobierno de Aragón (group E42_23R).

Conflicts of Interest

The authors declare no conflicts of interest.

References

1. R. Noyori, "Asymmetric Catalysis: Science and Opportunities (Nobel Lecture)," *Angewandte Chemie International Edition*41 (2002): 2008–2022.

2. R. H. Grubbs, "Olefin-Metathesis Catalysts for the Preparation of Molecules and Materials (Nobel Lecture)," *Angewandte Chemie International Edition* 45 (2006): 3760–3765.

3. A. Suzuki, "Cross-Coupling Reactions of Organoboranes: an Easy Way to Construct C-C Bonds (Nobel Lecture)," *Angewandte Chemie International Edition* 50 (2011): 6723–6737.

4. K. B. Sharpless, M. G. Finn, and H. C. Kolb, "Click Chemistry: The Certainty of Chance (Nobel Lecture)," *Angewandte Chemie International Edition* 64 (2025): e202501229.

5. A. J. Arduengo III and L. I. Iconaru, "Fused Polycyclic Nucleophilic Carbenes – Synthesis, Structure, and Function," *Dalton Transactions*, (2009): 6903–6914.

6. L. Benhamou, E. Chardon, G. Lavigne, S. Bellemin-Laponnaz, and V. César, "Synthetic Routes to N-Heterocyclic Carbene Precursors," *Chemical Reviews* 111 (2011): 2705–2733.

7. E. Peris, "Smart N-Heterocyclic Carbene Ligands in Catalysis," *Chemical Reviews* 118 (2018): 9988–10031.

8. Q. Zhao, G. Meng, S. P. Nolan, and M. Szostak, "N-Heterocyclic Carbene Complexes in C–H Activation Reactions," *Chemical Reviews* 120 (2020): 1981–2048.

9. P. Belotti, M. Koy, M. N. Hopkinson, and F. Glorius, "Recent Advances in the Chemistry and Applications of N-Heterocyclic Carbenes," *Nature Reviews Chemistry* 5 (2021): 711–725.

10. F. He, K. P. Zois, D. Tzeli, A. A. Danopoulos, and P. Braunstein, "N-Heterocyclic Carbenes as Bridgehead Donors in Metal Pincer Complexes," *Coordination Chemistry Reviews* 514 (2024): 215757.

11. S. S. Bera, G. Utecht-Jarzyńska, S. Yang, S. P. Nolan, and M. Szostak, "Metal–N-Heterocyclic Carbene Complexes in Buchwald–Hartwig Amination Reactions," *Chemical Reviews* 125 (2025): 5349–5435.

12. J. M. Praetorius and C. M. Crudden, "N-Heterocyclic Carbene Complexes of Rhodium: Structure, Stability and Reactivity," *Dalton Transactions* (2008): 4079–4094.

13. W. Gil and A. M. Trzeciak, "N-Heterocyclic Carbene–Rhodium Complexes as Catalysts for Hydroformylation and Related Reactions," *Coordination Chemistry Reviews* 255 (2011): 473–483.

14. M. Poyatos, G. Guisado-Barrios, and E. Peris, "N-Heterocyclic Carbenes: Effective Tools for Organometallic Synthesis" in book: "N-Heterocyclic carbenes," ed. S. P. Nolan (Wiley-VCH, 2014): 271–306.

15. V. César, L. H. Gade, and S. Bellemin-Laponnaz, "N-Heterocyclic Carbenes: From Laboratory Curiosities to Efficient Synthetic Tools," ch. 8, 2nd ed., ed. S. Díez-González (RSC Catalysis Series, 2017): 302–335.

16. J. Lee, H. Hahm, J. Kwak, and M. Kim "New Aspects of Recently Developed Rhodium(N-Heterocyclic Carbene)-Catalyzed Organic Transformations," *Advanced Synthesis & Catalysis* 361 (2019): 1479–1499.

17. E. van Vuuren, F. P. Malan, and M. Landman, "Multidentate NHC Complexes of Group IX Metals Featuring Carbon-Based Tethers: Synthesis and Applications," *Coordination Chemistry Reviews* 430 (2021): 213731.

18. W. A. Herrmann, J. Schütz, G. D. Frey, and E. Herdtweck, "N-Heterocyclic Carbenes: Synthesis, Structures, and Electronic Ligand Properties," *Organometallics* 25 (2006): 2437–2448.

19. M. V. Jiménez, J. J. Pérez-Torrente, M. I. Bartolomé, V. Gierz, F. J. Lahoz, and L. A. Oro, "Rhodium(I) Complexes with Hemilabile N-Heterocyclic Carbenes: Efficient Alkyne Hydrosilylation Catalysts," *Organometallics* 27 (2008): 224–234.

20. R. Savka and H. Plenio, "Facile Synthesis of [(NHC)MCl(cod)] and [(NHC)MCl(CO)2] (M=Rh, Ir) Complexes," *Dalton Transactions* 44 (2015): 891–893.

21. M. Bołt, L. Delaude, and P. Żak, "Rhodium Catalysts with Superbulky NHC Ligands for the Selective α-Hydrothiolation of Alkynes," *Dalton Transactions* 51 (2022): 4429–4434.

22. L. A. Turcio-García, H. Valdés, S. Hernández-Ortega, D. Canseco-Gonzalez, and D. Morales-Morales, "Arylation of Aldehydes Catalyzed by Fluorinated NHC–Rh(I) Complexes," *New Journal of Chemistry* 46 (2022): 16789–16800.

23. D. Kamzol, M. Bahramiveleshkolaei, and R. Wilhelm, "Camphor-Based NHC Ligands with a Sulfur Ligator Atom in Rhodium Catalysis: Catalytic Advances in the Asymmetric Ring Opening of N-Protected Azabenzonorbornenes," *Organic Letters* 27 (2025): 8417–8422.

24. R. Dorta, E. D. Stevens, and S. P. Nolan, "Double C-H Activation in a Rh-NHC Complex Leading to the Isolation of a 14-Electron Rh(III) Complex," *Journal of the American Chemical Society* 126 (2004): 5054–5055.

25. N. M. Scott, R. Dorta, E. D. Stevens, A. Correa, L. Cavallo, and S. P. Nolan, Interaction of a Bulky N-Heterocyclic Carbene Ligand with Rh(I) and Ir(I). Double C-H Activation and Isolation of Bare 14-Electron Rh(III) and Ir(III) Complexes, "*Journal of the American Chemical Society,*" 127 (2005): 3516–3526.

26. X.-Y. Yu, B. O. Patrick, and B. R. James, "Rhodium(III) Peroxo Complexes Containing Carbene and Phosphine Ligands," *Organometallics* 25 (2006): 4870–4877.

27. X.-Y. Yu, H. Sun, B. O. Patrick, and B. R. James, "N-Heterocyclic Carbene Rhodium Complexes and Their Reactions with H_2 and with CO," *European Journal of Inorganic Chemistry* 2009 (2009): 1752–1758.

28. O. V. Zenkina, E. C. Keske, R. Wang, and C. M. Crudden, "Double Single-Crystal-to-Single-Crystal Transformation and Small-Molecule Activation in Rhodium NHC Complexes," *Angewandte Chemie International Edition* 50 (2011): 8100–8104.

29. O. V. Zenkina, E. C. Keske, R. Wang, and C. M. Crudden, "Dimeric Rhodium−Ethylene NHC Complexes As Reactive Intermediates for the Preparation of Tetra-heteroleptic NHC Complexes," *Organometallics* 30 (2011): 6423–6432.

30. O. V. Zenkina, E. C. Keske, G. S. Kochhar, R. Wang, and C. M. Crudden, "Heteroleptic Rhodium NHC Complexes with Pyridine Derived Ligands: Synthetic Accessibility and Reactivity towards Oxygen," *Organometallics* 42 (2013): 2282–2293.

31. A. Di Giuseppe, R. Castarlenas, J. J. Pérez-Torrente, et al. "Ligand-Controlled Regioselectivity in the Hydrothiolation of Alkynes by Rhodium N-Heterocyclic Carbene Catalysts," *Journal of the American Chemical Society* 134 (2012): 8171–8183.

32. L. Palacios, M. J. Artigas, V. Polo, et al., "Hydroxo−Rhodium−N-Heterocyclic Carbene Complexes as Efficient Catalyst Precursors for Alkyne Hydrothiolation," *ACS Catalysis* 3 (2013): 2910–2919.

33. A. B. Chaplin, "Rhodium(I) Complexes of the Conformationally Rigid $IBioxMe_4$ Ligand: Preparation of Mono-, Bis-, and Tris-ligated NHC Complexes *Organometallics* 33 (2014): 3069–3077.

34. V. Varela-Izquierdo, J. A. López, B. de Bruin, C. Tejel, and M. A. Ciriano, "Three-Coordinate Rhodium Complexes in Low Oxidation States," *Chemistry – A European Journal* 26 (2020): 3270–3274.

35. K. J. Evans, P. A. Morton, C. Luz, et al., "Rhodium Indenyl NHC and Fluorenyl-Tethered NHC Half-Sandwich Complexes: Synthesis, Structures and Applications in the Catalytic C-H Borylation of Arenes and Alkanes," *Chemistry – A European Journal* 27 (2021): 17824–17833.

36. R. Azpíroz, M. O. Karataş, V. Passarelli, I. Özdemir, J. J. Pérez-Torrente, and R. Castarlenas, "Preparation of Mixed Bis-NHeterocyclic Carbene Rhodium(I) Complexes," *Molecules* 27 (2022): 7022.

37. R. Zhang, T. Yu, and G. Dong, "Rhodium Catalyzed Tunable Amide Homologation through a Hook-and-Slide Strategy," *Science* 382 (2023): 951–957.

38. S. Yang, T. Zhou, X. Yu, S. P. Nolan, and M. Szostak, "$[Pd(NHC)(\mu\text{-}Cl)Cl]_2$: The Highly Reactive Air- and Moisture-Stable, Well-Defined Pd(II)-N-Heterocyclic Carbene (NHC) Complexes for Cross-Coupling Reactions," *Accounts of Chemical Research* 57 (2024): 3343–3355.

39. A. Kapat, T. Sperger, S. Guven, and F. Schoenebeck, "E-Olefins through Intramolecular Radical Relocation," *Science* 363 (2019): 391–396.

40. J. A. Przyojski, K. P. Veggeberg, H. D. Arman, and Z. J. Tonzetich, "Mechanistic Studies of Catalytic Carbon−Carbon Cross-Coupling by Well-Defined Iron NHC Complexes," *ACS Catalysis* 5 (2015): 5938–5946.

41. G. A. Filonenko, M. J. B. Aguila, E. N. Schulpen, et al., "Bis-N-heterocyclic Carbene Aminopincer Ligands Enable High Activity in Ru-Catalyzed Ester Hydrogenation," *Journal of the American Chemical Society* 137 (2015): 7620–7623.

42. A. A. Danopoulos and P. Braunstein, "Mono-N-Heterocyclic Carbene Amido and Alkyl Complexes. Cobalt-Mediated C–H activation and C–C Coupling Reactions Involving Benzyl Ligands on a Putative 3-Coordinate Intermediate," *Dalton Transactions* 42 (2013): 7276–7280.

43. M. H. Al-Afyouni, V. M. Krishnan, H. D. Arman, and Z. J. Tonzetich, "Synthesis and Reactivity of Manganese(II) Complexes Containing N-Heterocyclic Carbene Ligands," *Organometallics* 34 (2015): 5088–5094.

44. F. Alonso, I. P. Beletskaya, and M. Yus, "Transition-Metal-Catalyzed Addition of Heteroatom-Hydrogen Bonds to Alkynes," *Chemical Reviews* 104 (2004): 3079–3159.

45. G. Cera and G. Maestri, "Palladium/Brønsted Acid Catalysis for Hydrofunctionalizations of Alkynes: From Tsuji-Trost Allylations to Stereoselective Methodologies," *ChemCatChem* 14 (2022): e202200295.

46. J. Chen, W.-T. Wei, Z. Lia, and Z. Lu, "Metal-Catalyzed Markovnikov-type Selective Hydrofunctionalization of Terminal Alkynes," *Chemical Society Reviews* 53 (2024): 7566–7589.

47. L. Huang, M. Arndt, K. Gooßen, H. Heydt, and L. J. Gooßen, "Late Transition Metal-Catalyzed Hydroamination and Hydroamidation," *Chemical Reviews* 115 (2015): 2596–2697.

48. T. Kondo, A. Tanaka, S. Kotachi, and Y. Watanabe "Ruthenium Complex-catalysed Addition of N-Aryl Substituted Amides to Alkynes: Novel Synthesis of Enamides," *Journal of the Chemical Society, Chemical Communications* (1995): 413–414.

49. L. J. Gooßen, J. E. Rauhaus, and G. Deng, "Ru-Catalyzed Anti-Markovnikov Addition of Amides to Alkynes: A Regio- and Stereoselective Synthesis of Enamides," *Angewandte Chemie, International Edition* 44 (2005): 4042–4045.

50. S. Yudha, Y. Kuninobu, and K. Takai, "Rhenium-Catalyzed Hydroamidation of Unactivated Terminal Alkynes: Synthesis of (E)-Enamides," *Organic Letters* 115 (2007): 5609–5611.

51. J.-F. Tan, C. T. Bormann, K. Severin, and N. Cramer, "Alkynyl Triazenes as Fluoroalkyne Surrogates: Regioselective Access to 4-Fluoro-2-pyridones by a Rh(III)-Catalyzed C−H Activation−Lossen Rearrangement−Wallach Reaction,"*ACS Catalysis* 10 (2020): 3790–3796.

52. X. Lyu, J. Zhang, D. Kim, S. Seo, and S. Chang, "Merging NiH Catalysis and Inner-Sphere Metal-Nitrenoid Transfer for Hydroamidation of Alkynes," *Journal of the American Chemical Society* 143 (2021): 5867–5877.

53. A. Bacchi, M. Costa, B. Gabriele, G. Pelizzi, and G. Salerno, "Efficient and General Synthesis of 5-(Alkoxycarbonyl)methylene-3-oxazolines by Palladium-Catalyzed Oxidative Carbonylation of Prop-2-ynylamides,"*The Journal of Organic Chemistry* 67 (2002): 4450–4457.

54. A. S. K. Hashmi, A. M. Schuster, and F. Rominger, "Gold Catalysis: Mild Conditions for the Synthesis of Oxazoles from N-Propargylcarboxamides and Mechanistic Aspects," *Organic Letters* 23 (2004): 4391–4394.

55. M. Breugst and H. Mayr, "Ambident Reactivities of Pyridone Anions," *Journal of the American Chemical Society* 132 (2010): 15380–15389.

56. M. W. Drover, J. A. Love, and L. L. Schafer, "1,3-N,O-Complexes of Late Transition Metals. Ligands with Flexible Bonding Modes and Reaction Profiles,"*Chemical Society Reviews* 46 (2017): 2913–2940.

57. A. Fedulin and A. Jacobi von Wangelin, , "2-Pyridonates: a Versatile Ligand Platform in 3d Transition Metal Coordination Chemistry and Catalysis," *Catalysis Science & Technology* 14 (2024): 26–42.

58. B. Español-Sánchez, J. Moradell, M. Galiana-Cameo, et al., "Ligand-Controlled Chemoselectivity in the Rhodium-Catalyzed Synthesis of Pentafulvenes via (2 + 2 + 1) Alkyne Cyclotrimerization," *Angewandte Chemie International Edition* 64 (2025): e202507424.

59. Y. H. Li, Y. Ouyang, J.-L. Yan, N. Chekshin, and J.-Q. Yu, "From Mono-N-Protected Amino Acids to Pyridones: A Decade of Evolution of Bifunctional Ligands for Pd(II)-Catalyzed C−H Activation," *Accounts of Chemical Research* 58 (2025): 2910–2926.

60. S.-W. Li, G. Wang, and Z.-S. Ye, "2-Hydroxypyridines as N- and O-Nucleophiles in Organic Synthesis," *European Journal of Organic Chemistry* 27 (2023): e202300998.

61. S. Meunier, J.-M. Siaugue, M. Sawicki, et al., "Modular Liquid-Phase Parallel Synthesis of a Highly Diverse Ligand Library," *Journal of Combinatorial Chemistry* 5 (2003): 201–204.

62. L. Mola, J. Font, L. Bosch, et al., "Nucleophile-Catalyzed Additions to Activated Triple Bonds. Protection of Lactams, Imides, and Nucleosides with MocVinyl and Related Groups," *The Journal of Organic Chemistry* 78 (2013): 5832–5842.

63. E. Petit, L. Bosch, J. Font, L. Mola, A. M. Costa, and J. Vilarrasa, "Tosvinyl and Besvinyl as Protecting Groups of Imides, Azinones, Nucleosides, Sultams, and Lactams. Catalytic Conjugate Additions to Tosylacetylene," *The Journal of Organic Chemistry* 79 (2014): 8826–8834.

64. B Weinstein and D. N. Brattesani, "The Reaction of Ethoxyacetylene with 2- and 4-Pyridone," *The Journal of Organic Chemistry* 32 (1967): 4107–4108.

65. L. A. Paquette, "Unsaturated Heterocyclic Systems. XVII.[1] The Reaction of 2(1H)-Pyridone with Hexafluoro-2-butyne," *The Journal of Organic Chemistry* 30 (1965): 2107–2108.

66. R. M. Acheson and P. A. Parker, "Addition Reactions of Heterocyclic Compounds. Part XXVII.[1] 2-Pyridones with Dimethyl Acetylenedicarboxylate," *Journal of the Chemical Society, Section C: Organic Chemistry* 61 (1967): 1542–1543.

67. R. Yadla, H. Rehman, J. M. Rao, and M. K. Mahesh, "Aromatic vs Diene Reactivityof 2(1H)-Pyridinone and its Derivatives," *Tetrahedron* 45 (1989): 7093–7098.

68. B. Mohtata, S. Jabbara, A. Ghasemia, and I. Yavari, "Synthesis of Alkyl 2-[2-oxopyridin-1(2H)-yl]acrylates by Nucleophilic Addition of Alkyl Propiolates Catalysed by Ph_3P," *Journal of Chemical Research* (2008): 601–603.

69. C.-J. Lu, D.-K. Chen, H. Chen, et al., "Palladium-Catalyzed Allylation of Tautomerizable Heterocycles with Alkynes," *Organic & Biomolecular Chemistry* 15 (2017): 5756–5763.

70. K. Wang, Z. Liu, G. Xu, et al., Chemo- and Enantioselective Insertion of Furyl Carbene into the N-H Bond of 2-Pyridones," *Angewandte Chemie International Edition,"* 60 (2021): 16942–16946.

71. S. Bera, A. Biswas, J. Pal, L. Roy, S. Mondal, and R. Samanta, "Pd(II)-Catalyzed Oxidative Naphthylation of 2-Pyridone through N−H/C−H Activation Using Diarylacetylene as an Uncommon Arylating Agent," *Organic Letters* 25 (2023): 1952–1957.

72. C. Li, M. Kähny, and B. Breit, "Rhodium-Catalyzed Chemo-, Regio-, and Enantioselective Addition of 2-Pyridones to Terminal Allenes," *Angewandte Chemie International Edition* 53 (2014): 13780–13784.

73. S. R. Sahoo and D. Sarkar, "Revisiting the Addition of in-situ Nucleophiles to Allenic Ketones: An Entry Towards Synthesis of Benzodioxins," *European Journal of Organic Chemistry* (2020): 1727–1731.

74. S. H. Park, J. Jang, K. Shin, and H. Kim, "Electrocatalytic Radical-Polar Crossover Hydroetherification of Alkenes with Phenols,"*ACS Catalysis* 12 (2022): 10572–10580.

75. M. Galiana-Cameo, R. Romeo, A. Urriolabeitia, et al., "Rhodium-NHC-Catalyzed gem-Specific O-Selective Hydropyridonation of Terminal Alkynes," *Angewandte Chemie International Edition* 61 (2022): e202117006.

76. B. Español-Sánchez, M. Galiana-Cameo, A. Urriolabeitia, et al., "Tuning the Pyridone Scaffold within a Rhodium-NHC Platform for gem-Specific Alkyne Dimerization via a Ligand-Assisted Proton Shuttle Mechanism," *Organometallics* 43 (2024): 2951–2962.

77. L. Palacios, A. Di Giuseppe, M. J. Artigas, et al., "Mechanistic Insight into the Pyridine Enhanced α-Selectivity in Alkyne Hydrothiolation Catalysed by Quinolinolate–Rhodium(I)–N-Heterocyclic Carbene Complexes," *Catalysis Science & Technology* 6 (2016): 8548–8561.

78. L. Palacios, Y. Meheut, M. Galiana-Cameo, et al., "Design of Highly Selective Alkyne Hydrothiolation RhI-NHC Catalysts: Carbonyl-Triggered Non-oxidative Mechanism," *Organometallics* 36 (2017): 2198–2207.

79. L. Rubio-Pérez, R. Azpíroz, A. Di Giuseppe, et al., "Pyridine-Enhanced Head-to-Tail Dimerization of Terminal Alkynes by a Rhodium–N-Heterocyclic-Carbene Catalyst,"*Chemistry – A European Journal* 19 (2013): 15304–15314.

80. R. Azpíroz, L. Rubio-Pérez, R. Castarlenas, J. J. Pérez-Torrente, and L. A. Oro, "Gem-Selective Cross-Dimerization and Cross-Trimerization of Alkynes with Silylacetylenes Promoted by a Rhodium–Pyridine–N-Heterocyclic Carbene Catalyst," *ChemCatChem* 6 (2014): 2587–2592.

81. M. Galiana-Cameo, M. Borraz, Y. Zelenkova, et al., "Rhodium(I)-NHC Complexes Bearing Bidentate Bis-Heteroatomic Acidato Ligands as gem-Selective Catalysts for Alkyne Dimerization," *Chemistry – A European Journal* 26 (2020): 9598–9608.

82. M. Galiana-Cameo, A. Urriolabeitia, E. Barrenas, et al.,"Metal–Ligand Cooperative Proton Transfer as an Efficient Trigger for Rhodium-NHC-Pyridonato Catalyzed gem-Specific Alkyne Dimerization," *ACS Catalysis* 11 (2021): 7553–7567.

83. M. O. Karataş, D. R. Hinojosa, V. Passarelli, L. A. Oro, J. J. Pérez-Torrente, and R. Castarlenas, "Rhodium(I) Complexes with Proton-Responsive Anionic Tethered N-Heterocyclic Carbene Ligands: Synthesis and Application in Alkyne Dimerization," *Dalton Transactions* 54 (2025): 15306–15319.

84. A. van Der Ent, A. L. Onderdelinden, and R. A. Schunn, "ChloroBis(Cyclooctene)Rhodium(I) and Iridium(I) Complexes," *Inorganic Syntheses* 14 (1973): 92–95.

85. K. V. Vasudevan, R. R. Butorac, C. D. Abernethy, and A. H. Cowley, "Synthesis and Coordination Compounds of a bis(imino)acenaphthene (BIAN)-Supported N-Heterocyclic Carbene," *Dalton Transactions* 39 (2010): 7401–7408.

86. A. J. Arduengo III, R. Krafczyk, R. Schmutzler, et al., "Imidazolylidenes, Imidazolinylidenes and Imidazolidines," *Tetrahedron* 55 (1999): 14523–14534.

87. G. Berthon-Gelloz, M. A. Siegler, A. L. Spek, B. Tinant, J. N. H. Reek, and I. E. Markó, "IPr* an Easily Accessible Highly Hindered N-Heterocyclic Carbene," *Dalton Transactions* 39 (2010): 1444–1446.

88. A. Gómez-Suárez, R. S. Ramón, O. Songis, A. M. Z. Slawin, C. S. J. Cazin, and S. P. Nolan, "Influence of a Very Bulky N-Heterocyclic Carbene in Gold-Mediated Catalysis," *Organometallics* 30 (2011): 5463–5470.

89. J. Huang, E. D. Stevens, and S. P. Nolan, "Intramolecular C-H Activation Involving a Rhodium-Imidazol-2-ylidene Complex and Its Reaction with H_2 and CO," *Organometallics* 19 (2000): 1194–1197.

90. S. Xu, K. Manna, A. Ellern, and A. D. Sadow, "Mixed N-Heterocyclic Carbene–Bis(oxazolinyl)borato Rhodium and Iridium Complexes in Photochemical and Thermal Oxidative Addition Reactions," *Organometallics* 33 (2014): 6840–6860.

91. E. Fooladi, B. Dalhus, and M. Tilset, "Synthesis and Characterization of Half-Sandwich N-Heterocyclic Carbene Complexes of Cobalt and Rhodium," *Dalton Transactions* 33 (2004): 3909–3917.

92. W. A. Herrmann, G. D. Frey, E. Herdtweck, and M. Steinbeck, "Synthesis and Characterization of N-Heterocyclic Carbene Substituted Phosphine and Phosphite Rhodium Complexes and their Catalytic Properties in Hydrogenation Reactions," *Advanced Synthesis & Catalysis* 349 (2007): 1677–1691.

93. A. Di Giuseppe, R. Castarlenas, J. J. Pérez-Torrente, F. J. Lahoz, and L. A. Oro, "Hydride-Rhodium(III)-N-Heterocyclic Carbene Catalysts for Vinyl-Selective H/D Exchange: A Structure–Activity Study," *Chemistry – A European Journal* 20 (2014): 8391–8403.

94. J.-N. Luy, S. A. Hauser, A. B. Chaplin, and R. Tonner, "Rhodium(I) and Iridium(I) Complexes of the Conformationally Rigid IBioxMe4 Ligand: Computational and Experimental Studies of Unusually Tilted NHC Coordination Geometries," *Organometallics* 34 (2015): 5099–5112.

95. J. M. Praetorius, R. Wang, and C. M. Crudden, "Structure and Reactivity of Dinitrogen Rhodium Complexes Containing N-Heterocyclic Carbene Ligands," *European Journal of Inorganic Chemistry* 2009 (2009): 1746–1751.

96. E. C. Keske, O. V. Zenkina, A. Asadi, et al., *Dalton Transactions*, "Dioxygen Adducts of Rhodium N-Heterocyclic Carbene Complexes," 42 (2013): 7414–7423.

97. L. Palacios, A. Di Giuseppe, R. Castarlenas, F. J. Lahoz, J. J. Pérez-Torrente, and L. A. Oro, "Pyridine versus Acetonitrile Coordination in Rhodium–N-Heterocyclic Carbene Square-Planar Complexes," *Dalton Transactions* 44 (2015): 5777–5789.

98. B. R. Van Ausdall, J. L. Glass, K. M. Wiggins, A. M. Aarif, and J. Louie, "Systematic Investigation of Factors Influencing the Decarboxylation of Imidazolium Carboxylates," *The Journal of Organic Chemistry* 74 (2009): 7935–7942.

99. A. J. Arduengo III, H. V. R. Dias, R. L. Harlow, and M. Kline, "Electronic Stabilization of Nucleophilic Carbenes," *Journal of the American Chemical Society* 114 (1992): 5530–5534.

100. W. A. Herrmann, C. Kocher, L. J. Gooßen, and G. R. J. Artus, "Heterocyclic Carbenes: A High-Yielding Synthesis of Novel, Functionalized N-Heterocyclic Carbenes in Liquid Ammonia," *Chemistry – A European Journal* 2 (1996): 1627–1636.

101. Q. Liang, K. Sheng, A. Salmon, V. Y. Zhou, and D. Song, "Active Iron(II) Catalysts toward gem-Specific Dimerization of Terminal Alkynes," *ACS Catalysis* 9 (2019): 810–818.

102. M. O. Karataş, A. Di Giuseppe, V. Passarelli, et al., "Pentacoordinated Rhodium(I) Complexes Supported by Coumarin-Functionalized N-Heterocyclic Carbene Ligands," *Organometallics* 37 (2018): 191–202.

103. A. Srinivasan, J. Campos, N. Giraud, M. Robert, and O. Rivada-Wheelaghan, "Mn(I) Complex Redox Potential Tunability by Remote Lewis Acid Interaction," *Dalton Transactions* 49 (2020): 16623–16626.

104. C. Lohre, T. Dröge, C. Wang, and F. Glorius, "Nickel-Catalyzed Cross-Coupling of Aryl Bromides with Tertiary Grignard Reagents Utilizing Donor-Functionalized N-Heterocyclic Carbenes (NHCs)," *Chemistry – A European Journal* 17 (2011): 6052–6055.

105. G. Cavallo, P. Metrangolo, R. Milani, et al., "The Halogen Bond," *Chemical Reviews* 116 (2016): 2478–2601.

106. B. K. Saha, R. V. P. Veluthaparambath, and G. V. Krishna, "Halogen…Halogen Interactions: Nature, Directionality and Applications," *Chemistry, An Asian Journal* 18 (2023): e202300067.

107. S. J. Grabowski, "Halogen Bonds with Carbenes Acting as Lewis Base Units: Complexes of Imidazol-2-ylidene: Theoretical Analysis and Experimental Evidence," *Physical Chemistry Chemical Physics* 25 (2023): 9636–9647.

108. F. Izquierdo, S. Manzini, and S. P. Nolan, "The Use of the Sterically Demanding IPr* and Related Ligands in Catalysis," *Chemical Communications* 50 (2014): 14926–14937.

109. J. Diesel, A. M. Finogenova, and N. Cramer, "Nickel-Catalyzed Enantioselective Pyridone C–H Functionalizations Enabled by a Bulky N-Heterocyclic Carbene Ligand," *Journal of the American Chemical Society* 140 (2018): 4489–4493.

110. M. Bołt and P. Żak, "Application of Bulky NHC–Rhodium Complexes in Efficient S–Si and S–S Bond Forming Reactions," *Inorganic Chemistry* 60 (2021): 17579–17585.

111. X. Xu, C. Gourlaouen, B. Jacques, and S. Dagorne, "Robust Two-Coordinate Zn(II) Organocations Supported by Bulky- Yet-Flexible IPr* Carbene: Synthesis, Structure, and Distinct Reactivity in Hydrosilylation Catalysis," *Organometallics* 42 (2023): 2813–2825.

112. K. J. Brick, M. Q. Lim, and E. C. Keske, "[(NHC)Pd(allyl)Cl] Precatalysts in The Hiyama Reaction of Aryl Chlorides with Aryl Trimethoxysilanes: A Study in Side Reactions," *Organometallics* 42 (2023): 3192–3198.

113. K. Halikowska-Tarasek, W. Ochędzan-Siodłak, B. Dziuk, R. Szostak, M. Szostak, and E. Bisz, "IPr*diNHC: Sterically Adaptable Dinuclear N-Heterocyclic Carbenes," *Inorganic Chemistry* 64 (2025): 7851–7857.

114. Q. Teng and H. V. Huynh, "A Unified Ligand Electronic Parameter Based on ^{13}C NMR Spectroscopy of N-Heterocyclic Carbene Complexes," *Dalton Transactions* 46 (2017): 614–627.

115. C. Chen, F.-S. Liu, and M. Szostak, "BIAN-NHC Ligands in Transition-Metal-Catalysis: A Perfect Union of Sterically Encumbered, Electronically Tunable N-Heterocyclic Carbenes?," *Chemistry – A European Journal* 27 (2021): 4478–4499, and references therein.

116. J. Li, C. Huang, D. Wen, Q. Zheng, B. Tu, and T. Tu, "Nickel-Catalyzed Amination of Aryl Chlorides with Amides," *Organic Letters* 23 (2021): 687–691.

117. R. Fan, M. Kuai, D. Lin, F. Bauer, and W. Fang, "A General C–N Cross-Coupling to Synthesize Heteroaryl Amines Using a Palladacyclic N-Heterocyclic Carbene Precatalyst," *Organic Letters* 24 (2022): 8688–8693.

118. J. Zhang, T. Li, X. Li, et al., "An Air-Stable, Well-Defined Palladium–BIAN–NHC Chloro Dimer: a Fast-Activating, Highly Efficient Catalyst for Cross-Coupling," *Chemical Communications* 58 (2023): 7404–7407.

119. D. J. Nelson and S. P. Nolan, "Quantifying and Understanding the Electronic Properties of N-Heterocyclic Carbenes," *Chemical Society Reviews* ,47 (2013): 6723–6756.

120. H. V. Huynh, "Electronic Properties of N-Heterocyclic Carbenes and Their Experimental Determination," *Chemical Reviews* 118 (2018): 9457–9492.

121. F. Bru, R. S. C. Charman, L. Bourda, et al., "A Simply Accessible Organometallic System to Gauge Electronic Properties of N-Heterocyclic Carbenes," *Dalton Transactions* 53 (2024): 16030–16037.

122. Q. Cao, W. I. Nicholson, A. C. Jones, and D. L. Browne, "Robust Buchwald–Hartwig Amination Enabled by Ball-Milling," *Organic & Biomolecular Chemistry* 17 (2019): 1722–1726.

123. V. M. Chernyshev, E. A. Denisova, D. B. Eremin, and V. P. Ananikov, "The Key Role of R–NHC Coupling (R = C, H, Heteroatom) and M–NHC Bond Cleavage in the Evolution of M/NHC Complexes and Formation of Catalytically Active Species," *Chemical Science* 11 (2020): 6957–6977.

124. R. O. Pankov, D. O. Prima, and V. P. Ananikov, "Tailoring Metal Complexes with N-Heterocyclic Carbene Ligands Using Electron-Withdrawing Groups: Impact on Catalytic Activity and Property Development," *Coordination Chemistry Reviews* 516 (2024): 215897.

125. SAINT+, *Area-Detector Integration Software, version 6.01* (Bruker AXS, 2001).

126. G. M. Sheldrick, *SADABS Program* (University of Göttingen, 1999).

127. G. M. Sheldrick, *SHELXS* (University of Göttingen 97, 1997).

128. G. M. Sheldrick, "Crystal Structure Refinement with SHELXL," *Acta Crystallographica Section C: Structural Chemistry* 71 (2015): 3–8.

129. L. J. Farrugia, "WinGX and ORTEP for Windows: An Update," *Journal of Applied Crystallography* 45 (2012): 849–854.

130. R. Azpíroz, R. L.Rubio-Pérez, A. Di Giuseppe, et al., "Rhodium(I)-N-Heterocyclic Carbene Catalyst for Selective Coupling of N-Vinylpyrazoles with Alkynes via C–H Activation," *ACS Catalysis* 4 (2014): 4244–4253.

Supporting Information

Additional supporting information can be found online in the Supporting Information section. **Supporting Fig. S1:** ^{1}H NMR spectrum of **2** in THF-d_8 at 243 K. **Supporting Fig. S2:** ^{13}C{^{1}H}-APT NMR spectrum of **2** in THF-d_8 at 243 K. **Supporting Fig. S3:** ^{1}H-^{1}H COSY NMR spectrum of **2** in THF-d_8 at 243 K. **Supporting Fig. S4:** ^{1}H-^{13}C HSQC NMR spectrum of **2** in THF-d_8 at 243 K. **Supportng Fig. S5:** ^{1}H-^{13}C HMBC NMR spectrum of **2** in THF-d_8 at 243 K. **Supporting Fig. S6:** ^{1}H NMR spectrum of **3** in toluene-d_8 at 253 K. **Supporting Fig. S7:** ^{13}C{^{1}H}-APT NMR spectrum of 3 in toluene-d_8 at 253 K. **Supporting Fig. S8:** ^{1}H-^{1}H COSY NMR spectrum of **3** in toluene-d_8 at 253 K. **Supporting Fig. S9:** ^{1}H-^{13}C HSQC NMR spectrum of **3** in toluene-d_8 at 253 K. **Supporting Fig. S10:** ^{1}H-^{13}C HMBC NMR spectrum of **3** in toluene-d_8 at 253 K. **Supporting Fig. S11:** ^{1}H NMR spectrum of **4** in THF-d_8 at 298 K. **Supporting Fig. S12:** ^{13}C{^{1}H}-APT NMR spectrum of **4** in THF-d_8 at 298 K. **Supporting Fig. S13:** ^{1}H-^{1}H COSY NMR spectrum of **4** in THF-d_8 at 298 K. **Supporting Fig. S14:** ^{1}H-^{13}C HSQC NMR spectrum of **4** in THF-d_8 at 298 K. **Supporting Fig. S15:** ^{1}H-^{13}C HMBC NMR spectrum of **4** in THF-d_8 at 298 K. **Supporting Fig. S16:** ^{1}H-^{1}H 2D-NOESY NMR spectrum of **4** in THF-d_8 at 298 K. **Supporting Fig. S17:** ^{1}H NMR spectrum of **6** in toluene-d_8 at 253 K. **Supporting Fig. S18:** ^{13}C{^{1}H}-APT NMR spectrum of **6** in toluene-d_8 at 253 K. **Supporting Fig. S19:** ^{1}H-^{1}H COSY NMR spectrum of **6** in toluene-d_8 at 253 K. **Supporting Fig. S20:** ^{1}H-^{13}C HSQC NMR spectrum of **6** in toluene-d8 at 253 K. **Supporting Fig. S21:** ^{1}H-^{13}C HMBC NMR spectrum of 6 in toluene-d_8 at 253 K. **Supporting Fig. S22:** ^{1}H-^{1}H 2D-NOESY NMR spectrum of **6** in toluene-d_8 at 253 K. **Supporting Fig. S23:** ^{1}H NMR spectrum of **7** in C6D6 at 298 K. **Supporting Fig. S24:** ^{13}C{^{1}H}-APT NMR spectrum of **7** in C_6D_6 at 298 K. **Supporting Fig. S25:** ^{1}H-^{1}H COSY NMR spectrum of **7** in C_6D_6 at 298 K. **Supporting Fig. S26:** ^{1}H-^{13}C HSQC NMR spectrum of **7** in C_6D_6 at 298 K. **Supporting Fig. S27:** ^{1}H-^{13}C HMBC NMR spectrum of **7** in C_6D_6 at 298 K. **Supporting Fig. S28:** ^{1}H NMR spectrum of **8** in C_6D_6 at 298 K. **Supporting Fig. S29:** ^{13}C{^{1}H}-APT NMR spectrum of **8** in C_6D_6 at 298 K. **Supportng Fig. S30:** ^{1}H-^{1}H COSY NMR spectrum of **8** in C_6D_6 at 298 K. **Supporting Fig. S31:** ^{1}H-^{13}C HSQC NMR spectrum of **8** in C_6D_6 at 298 K. **Supporting Fig. S32:** ^{1}H-^{13}C HMBC NMR spectrum of **8** in C_6D_6 at 298 K.